

1

Electronic Supporting Information (ESI)

2 Surfactin functionalized poly(methyl methacrylate) as eco-friendly nano-adsorbent: from size
3 controlled scalable fabrication to adsorptive removal of inorganic and organic pollutants

4 Debasree Kundu^{a,‡}, Chinmay Hazra^{a,‡}, Aniruddha Chatterjee^{b,*}, Ambalal Chaudhari^a,
5 Satyendra Mishra^b, Amol Kharat^c and Kiran Kharat^d

6 *^aSchool of Life Sciences, North Maharashtra University, Jalgaon, Maharashtra, India*

7 *^bUniversity Institute of Chemical Technology, North Maharashtra University, Jalgaon,*
8 *Maharashtra, India*

9 *^cModern College of Pharmacy, Moshi, Pune, Maharashtra, India*

10 *^dDepartment of Biotechnology, Deogiri college, Aurangabad, Maharashtra, India*

11

12

13

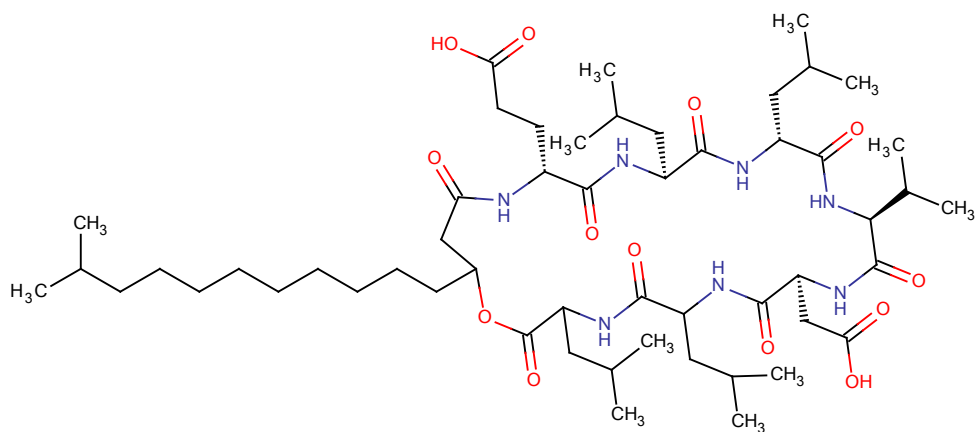
14

15

16

17 *Corresponding author. Present address: Maharashtra Institute of Technology, Aurangabad,
18 Maharashtra, India. E-mail: aniruddha_chatterjee2006@yahoo.co.in;
19 aniruddha.chatterjee@mit.asia

20 ‡These authors contributed equally as first authors in this manuscript



1

2 **Fig. S1.** Overall chemical structure of surfactin lipopeptide.

3

Determination of monomer conversion, solid content, molecular weights and polydispersity index (PDI)

The percentage of monomer conversion to polymer and latex yield was determined by gravimetric analysis. A small sample (5-10 ml) was taken and placed quickly into a capped vial containing several drops of hydroquinone inhibitor solution to stop the polymerization. The sample was then poured into a pre-weighed watch glass and weighed. It was then dried in an oven at 120 °C until constant weight. A final measurement of the watch glass + dry polymer sample was then made. For each set of operating conditions, experiments were repeated and the repeatability of measurements was within $\pm 10\%$, as indicated by error bars on the graphical plots.

The total number of latex particles in the system (N_p) and the number of polymer chains per particle (N) as well as the conversion (X_m) are calculated according to the following equations:

$$N_p = \frac{6\rho_0 V X_m}{\rho \pi D^3} \quad (1)$$

$$N = \frac{4}{3} \frac{\rho \pi (D/2)^3 N_A}{M_n} \quad (2)$$

$$X_m (\%) = \frac{W_1}{W_2} \times 100 \quad (3)$$

where ρ_0 is the density of MMA (0.94 g cm⁻³ at 25 °C), V is the total volume of MMA, X_m is polymerization conversion, ρ is the density of PMMA (g cm⁻³ at 25 °C), D is the diameter of the particle, N_A is 6.02×10^{23} mol⁻¹, M_n is the number-average molecular weight, and W_1 and W_2 are the weights of the polymer and MMA, respectively.

Energy calculations

1. Energy delivered during conventional mechanically stirred emulsion polymerization method

Voltage input in magnetic stirrer = 230 V.

Current measured using digital multimeter (Model 801, Mecco Instruments Pvt. Ltd., India) = 37 mA = 37×10^{-3} A.

Power input in overhead stirrer = voltage input \times current measured = 230 (V) \times 37×10^{-3} (A) = 8.51 W (J/s).

Time required for completion of reaction = 1 h (3600 s).

Net energy delivered during conventional method = power input in magnetic stirrer \times time required for completion of reaction = 8.51 J/s \times 3600 s = 30636 J = 30.636 kJ.

Energy supplied in form of heat to maintain reaction temperature 55 °C = $mC_{p, \text{mix}} (T_{\text{process}} - T_{\text{ref}})$ = $130.38 \times 4.0058 \times (55 - 25)$ = 15668.3 J = 15.67 kJ.

Total energy supplied during conventional method = 30.636 + 15.67 = 46.31 kJ.

Quantity of material processed = quantity of [water + KPS + surfactin + MMA] = 100 ml + 0.25 g + 0.025 g + 5 g = 105.28 g.

Net energy supplied for processing of material using conventional method = net energy delivered during conventional method/quantity of material processed = 46.31 (kJ) / 105.28 (g) = 43.98×10^{-2} (kJ/g). (A)

2. Energy delivered during sonochemical polymerization

Energy delivered during sonication = energy required to synthesize nPMMA.

Electrical energy delivered during sonication (indicated by the power meter) = 53.5 kJ.

Efficiency of horn taken for the calculation = 18.9% (estimated independently using calorimetric studies).

Actual energy delivered by horn during sonication = energy delivered during sonication using horn \times efficiency of horn = $53.5 \times 18.9/100 = 10.11$ kJ.

Quantity of material processed = quantity of [water + KPS + surfactin + MMA] = 100 ml + 0.25 g + 0.025 g + 5 g = 105.28 g.

Net energy supplied for processing of material using sonochemical method = actual energy delivered by horn during sonication/quantity of material processed = 10.11 (kJ) / 105.28 (g) = 9.60×10^{-2} (kJ/g). (B)

3. Energy saved

Net energy saved = [net energy supplied for processing of material using atomized microemulsion method (A)] - [net energy supplied for processing of material using sonochemical emulsion polymerization (B)] = 43.98×10^{-2} (kJ/g) - 9.60×10^{-2} (kJ/g) = 34.38×10^{-2} (kJ/g).

Calculation of cavitation yield

1. Conventional mechanically stirred emulsion polymerization

Rate of polymerization = 1.26 g l⁻¹

Power density (J l⁻¹) = supplied total electrical energy = 46.31 kJ = 46310 J l⁻¹

Cavitation yield = 1.26 (g l⁻¹) / 46310 (J l⁻¹) = 0.27×10^{-4} g J⁻¹

2. sonochemical polymerization

Rate of polymerization = 1.51 g l⁻¹

Power density (J l⁻¹) = supplied total electrical energy = 10.11 kJ = 10110 J l⁻¹

Cavitation yield = 1.51 (g l⁻¹) / 10110 (J l⁻¹) = 1.5×10^{-4} g J⁻¹

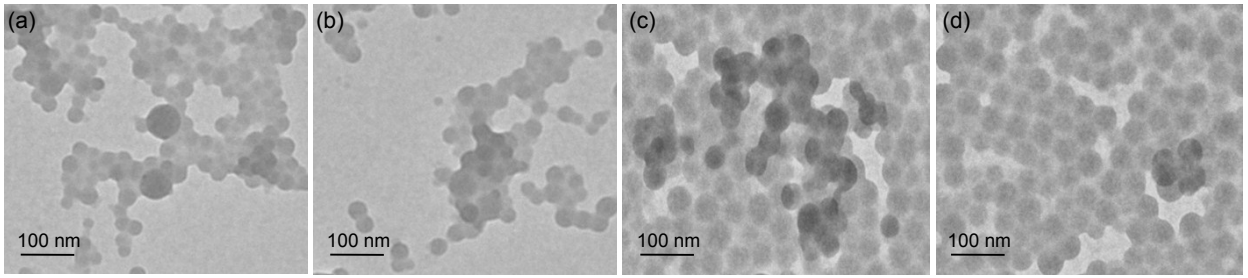


Fig. S2. Effect of surfactin concentration (wt. % of MMA) on morphology and size of nPMMA_{SP} particles: (a) 1%, (b) 2%, (c) 3% and (d) 4%. Other conditions are same as Fig. 1.

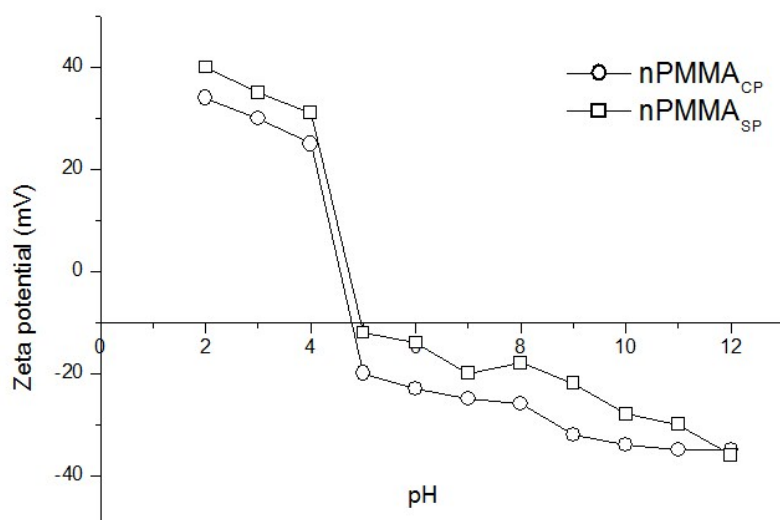


Fig. S3. The pH dependence of zeta-potential of nPMMA_{SP} and nPMMA_{CP} particles. (Reaction conditions: nPMMA_{SP}: monomer-to-water 20 wt.%; monomer-to-initiator 0.4 wt.%; surfactin 4 wt.%, calculated vs monomer; temperature, 55±2 °C; time, 1 h; nPMMA_{CP}: monomer-to-water 20 wt.%; monomer-to-initiator 0.4 wt.%; surfactin 4 wt.%, calculated vs monomer; temperature, 55±2 °C; agitation, 250 rpm; time, 1 h).

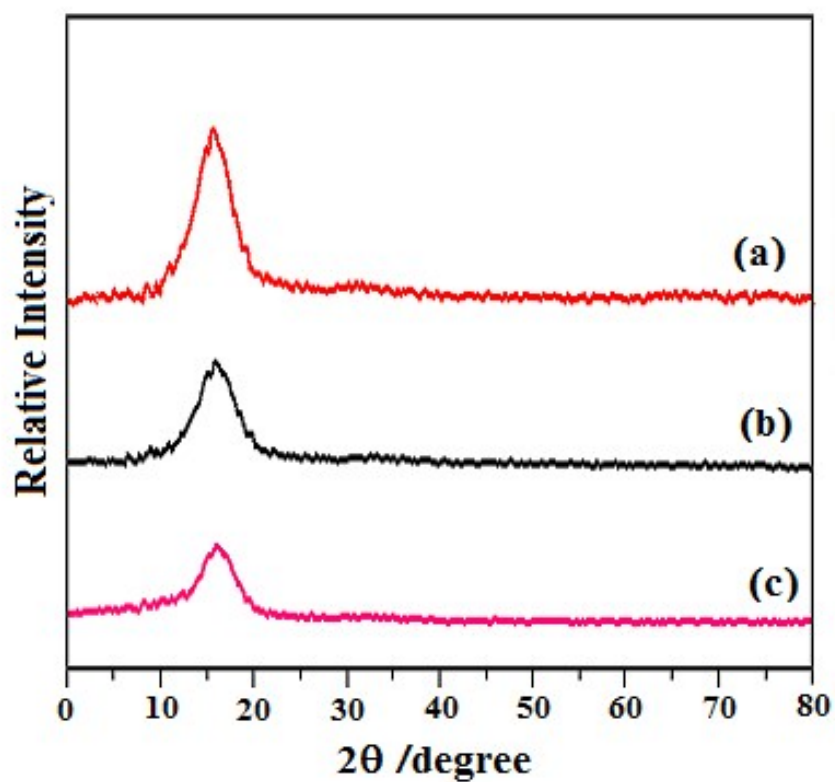


Fig. S4. XRD patterns of (a) nPMMA_{SP}, (b) nPMMA_{CP} and (c) bulk PMMA.

The diffraction peak observed at 15.10° was assigned to the amorphous phase of PMMA. This peak was more prominent in nPMMA_{SP}. It suggested the crystalline nature of nPMMA_{SP} was more than nPMMA_{CP} and bulk PMMA.

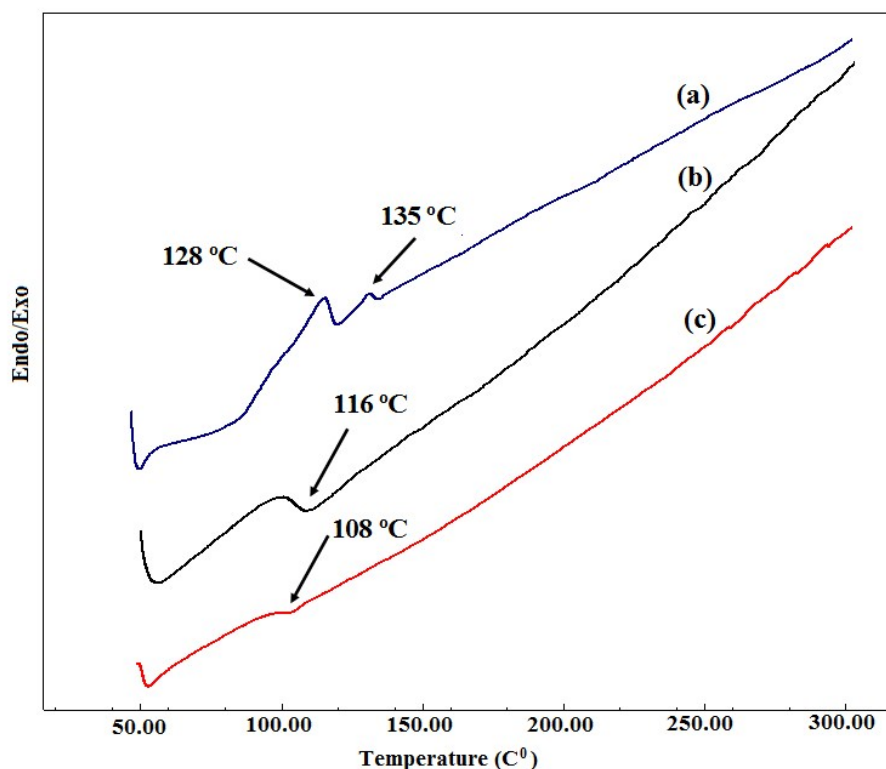


Fig. S5. DSC curves of (a) nPMMA_{SP} and (b) nPMMA_{CP} and (c) bulk PMMA.

It was observed that first scan of nPMMA_{SP} showed two step exothermic peaks at 128 and 135 °C that were attributed to T_{g1} along with respective peaks of T_m arising due to the presence of little amount of surfactin (Fig. S5a). This finding corroborated with the thin shell layer of biosurfactants observed in TEM. The lower value of T_{g1} (Fig. S5b) for nPMMA_{CP} (116 °C) was due to its relatively large size and lower surface area as compared to nPMMA_{SP}. Moreover, the peak for surfactin shell could not be detected due to poor grafting of surfactin onto nPMMA in case of nPMMA_{CP}. Bulk PMMA showed regular T_g at 108 °C like commercial grade PMMA (Fig. S5c). The reason for high T_g of polymer nanoparticles than bulk PMMA might be a decrease in particle size to nano-scale that results in an increase in surface area and higher surface energy.

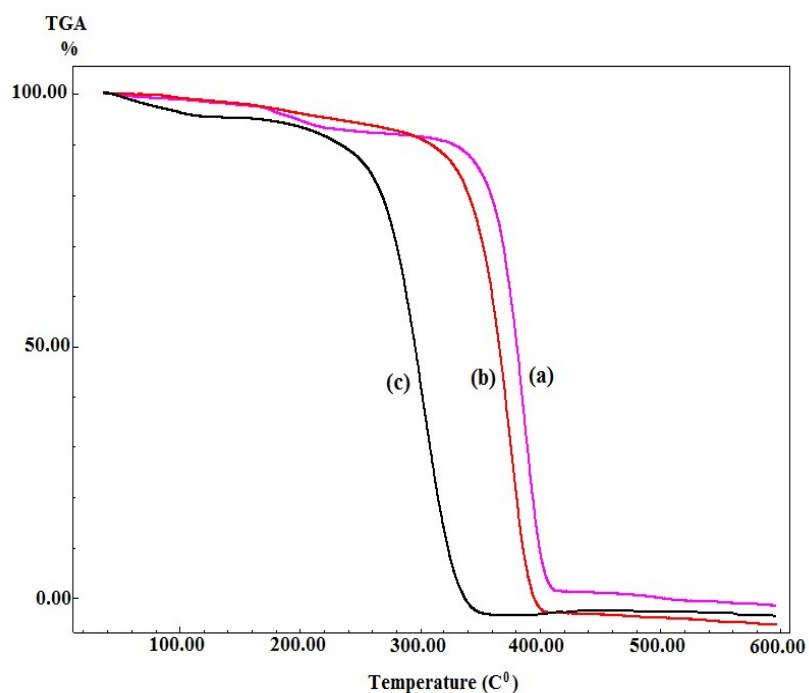


Fig. S6. TGA thermogram of (a) nPMMA_{SP} and (b) nPMMA_{CP} and (c) bulk PMMA.

A remarkable change in thermal behaviour between nPMMA_{SP}, nPMMA_{CP} and bulk PMMA was observed. The nPMMA_{SP} showed higher thermal stability [$d_{on} = 372$ °C and $d_{off} = 415$ °C with % weight loss (W_L) = 100%] than nPMMA_{CP} [$d_{on} = 352$ °C and $d_{off} = 406$ °C with % weight loss (W_L) = 100%] and bulk PMMA [$d_{on} = 282$ °C and $d_{off} = 356$ °C with 100% W_L]. Thus, the thermal stability pattern followed the order: nPMMA_{SP} > nPMMA_{CP} > bulk PMMA.

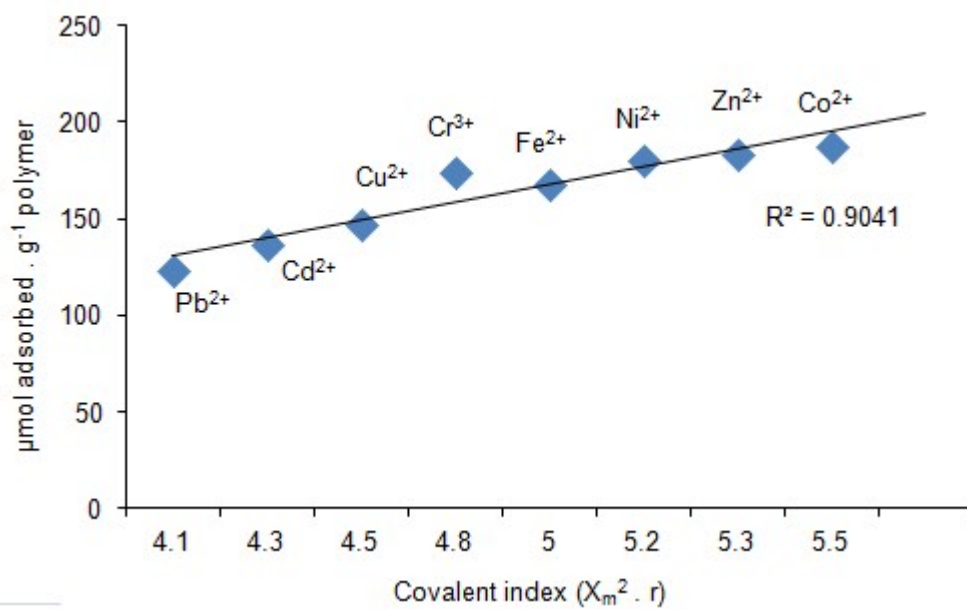


Fig. S7. Plot of the adsorption capacities against the covalent indices.

Parameter	Setting
λ	130 nm to 770 nm
RF Power	1300 W
Nebulizer	Low flow
Plasma Flow	15 l min ⁻¹
Auxiliary Flow	0.2 l min ⁻¹
Nebulizer Flow	0.8 l min ⁻¹
Pump Rate/ Sample Flow	1.5 ml min ⁻¹
Spray Chamber	HF resistant cyclonic
Integration Time	10-20 seconds
Number of replicates	3

Table S1. ICP-AES instrumental operating parameters used for the determination of potentially toxic metals binding to nano-adsorbents used in this study.

Run	MMA:KPS (wt.%)	Solid content (%)	t^*_{blue} (min)	Particle size (nm)		Polydispersity index	$N_p \times 10^{18}$	N
				DLS	TEM			
Sonochemical emulsion polymerization								
1	0.0	12.171±0.122	11	218.137±6.554	180.011±10.550	0.952±0.012	0.913±0.552	11
2	0.1	13.153±0.321	09	138.662±11.833	106.557±10.322	0.741±0.066	3.935±0.116	23
3	0.2	14.155±0.116	07	139.538±6.115	105.086±10.555	0.894±0.092	4.664±0.562	24
4	0.3	16.882±0.344	07	104.512±8.831	81.055±7.510	0.732±0.122	6.317±0.124	21
5	0.4	27.534±0.217	04	75.421±2.832	60.225±1.511	0.554±0.092	7.883±0.323	14
6	0.5	18.682±0.217	06	90.554±7.894	79.522±1.833	0.911±0.166	7.032±0.339	19
7	1.0	17.152±0.143	06	79.552±11.446	73.625±1.723	0.655±0.124	6.964±0.321	18
8	1.5	25.551±0.222	05	72.511±10.871	63.512±3.476	0.727±0.164	6.551±0.552	14
9	2.0	22.155±0.344	05	76.025±5.112	64.533±4.222	0.643±0.088	4.877±0.803	15
10	3.0	21.693±0.255	04	75.523±3.835	66.216±3.821	0.592±0.074	3.714±0.221	17
Conventional polymerization (with mechanical stirring)								
1	0.0	11.142±0.124	14	229.025±12.912	190.088±7.444	0.973±0.088	0.855±0.188	13
2	0.1	12.571±0.361	12	155.013±10.225	125.057±12.875	0.752±0.071	3.143±0.255	21
3	0.2	13.144±0.112	11	131.085±7.287	110.024±10.514	0.806±0.150	3.618±0.624	20
4	0.3	14.856±0.333	09	110.511±9.132	85.533±6.527	0.711±0.033	5.511±0.255	23
5	0.4	25.554±0.242	07	79.533±2.562	72.341±3.522	0.632±0.061	6.722±0.511	12
6	0.5	18.682±0.114	07	95.542±2.830	80.066±3.555	0.875±0.075	6.777±0.222	21
7	1.0	16.551±0.211	08	100.016±8.732	85.042±5.425	0.633±0.177	5.854±0.541	25
8	1.5	22.554±0.224	05	90.088±6.656	82.552±6.138	0.633±0.055	6.183±0.207	15
9	2.0	21.133±0.313	05	95.035±8.555	90.086±13.565	0.662±0.021	4.537±0.212	18
10	3.0	20.652±0.115	05	135.017±8.937	116.211±11.558	0.697±0.044	3.653±0.443	14

*: the time when the colour of the microemulsion turns blue

Table S2. Effect of monomer-to-initiator weight ratios on particle size, PDI, conversion, N_p and N of the particles. Conditions are as in Fig. 1.

Run	MMA:water (wt.%)	Particle size (nm)		Polydispersity index	$N_p \times 10^{18}$	N
		DLS	TEM			
Sonochemical emulsion polymerization						
1	5	88.542	66.521	0.622	6.783	14
2	10	119.515	85.017	0.721	6.557	14
3	15	114.553	90.044	0.713	5.883	15
3	20	79.016	60.027	0.552	7.612	13
Conventional polymerization (with mechanical stirring)						
1	5	90.557	68.066	0.657	7.004	16
2	10	111.525	85.549	0.705	7.222	17
3	15	115.578	92.026	0.754	7.254	18
4	20	75.055	73.022	0.613	7.102	15

Table S3. Effect of MMA concentration on particle size, PDI, conversion, N_p and N of the particles. Other conditions are same as Fig. 1.

Run	Acoustic amplitude (%)	Energy input (kJ)	Actual power dissipated (P , W) (measured calorimetrically)	Power input per unit volume (kW/m^3)	Efficiency (%)	Particle size (nm)		Polydispersity index	$N_p \times 10^{18}$	N	Conversion (%)
						DLS	TEM				
1	30	23.811	22.112	497.944	9.212	220.544	182.077	0.981	0.922	10	67.055
2	40	36.215	31.433	751.552	13.111	130.532	103.036	0.745	3.963	22	77.112
3	50	53.522	45.543	1136.841	18.967	79.511	60.044	0.553	7.632	13	91.233
4	65	67.717	60.022	1413.514	25.055	120.043	83.052	0.752	6.251	20	85.355
5	70	77.118	65.054	1607.504	27.183	105.022	75.513	0.663	6.573	19	81.088

Table S4. Effect of acoustic amplitude on particle size, PDI, conversion, N_p and N of nPMMA_{SP} particles.

Run	Wt. % biosurfactant (of MMA)	Particle size (nm)		Polydispersity index	$N_p \times 10^{18}$	N
		DLS	TEM			
Sonochemical emulsion polymerization						
1	1.0	120.077	85.027	0.704	5.544	14
2	2.0	90.022	67.512	0.632	6.751	14
3	3.0	110.037	82.044	0.734	6.613	13
4	4.0	85.054	60.036	0.572	7.577	14
Conventional polymerization (with mechanical stirring)						
1	1.0	120.022	85.082	0.791	6.233	17
2	2.0	90.016	67.555	0.651	7.264	15
3	3.0	110.052	82.023	0.762	7.172	18
4	4.0	85.073	70.516	0.513	6.735	14

Table S5. Effect of surfactin concentration on particle size, PDI, conversion, N_p and N of the particles. Other conditions are same as Fig. 1.

Model	Parameters	Co²⁺	Zn²⁺	Ni²⁺	Cr³⁺
Pseudo-first-order	k_1 (min ⁻¹)	0.038	0.045	0.044	0.032
	$q_{e,calc}$ (mg g ⁻¹)	30.155	28.463	27.434	34.141
	R^2	0.943	0.947	0.935	0.953
	$RMSE$	0.031	0.024	8.652	0.814
	$ERRSQ$	0.242	0.173	63.303	6.431
Pseudo-second-order	k_2 (g mg ⁻¹ min ⁻¹)	0.624	0.914	0.137	0.532
	$q_{e,calc}$ (mg g ⁻¹)	34.656	34.022	31.552	44.088
	R^2	0.998	0.999	0.999	0.994
	$RMSE$	0.016	0.003	0.812	0.748
	$ERRSQ$	0.117	0.034	6.455	6.582
Elovich	α (mg g ⁻¹ min ⁻¹)	5.69E + 24	1.66E + 28	68.4162	3314.526
	β (g mg ⁻¹)	28.572	27.863	6.983	27.114
	R^2	0.932	0.956	0.986	0.991
	$RMSE$	0.085	0.039	6.372	6.831
	$ERRSQ$	0.689	0.477	8.105	6.214
Intraparticle diffusion	k_d (mg g ⁻¹ min ^{-0.5})	0.005	0.008	0.037	0.014
	C (mg g ⁻¹)	30.683	32.111	30.473	43.572
	R^2	0.974	0.982	0.955	0.962
	$RMSE$	0.027	0.082	3.178	5.166
	$ERRSQ$	0.587	0.325	8.144	6.024

Table S6. Kinetic model parameters and error function data for the metal ions sorption onto nPMMA_{SP} particles.

Isotherms	Parameters	Co²⁺	Zn²⁺	Ni²⁺	Cr³⁺
Langmuir	Q_0 (mg g ⁻¹)	24.573	25.857	27.843	36.479
	K_L (l mg ⁻¹)	0.044	0.031	0.038	0.042
	R^2	0.904	0.895	0.937	0.983
	$RMSE$	0.066	0.012	0.568	0.552
	$ERRSQ$	0.311	0.432	3.558	2.637
Freundlich	K_F	7.471	5.213	4.332	4.884
	$1/n$	0.532	0.441	0.383	0.414
	R^2	0.927	0.958	0.962	0.902
	$RMSE$	0.088	0.853	1.274	1.548
	$ERRSQ$	10.889	2.442	3.769	2.551
Temkin	b_T	9.664	8.892	6.432	9.221
	A_T (l g ⁻¹)	1.183	2.122	0.443	0.522
	R^2	0.933	0.944	0.921	0.922
	$RMSE$	0.042	0.017	0.441	0.502
	$ERRSQ$	0.818	0.779	1.764	3.374
Redlich-Peterson	K_R (l g ⁻¹)	0.781	1.374	4.733	5.662
	a_R (mg ⁻¹)	0.055	0.132	0.035	0.042
	g	10.221	0.834	0.942	0.785
	R^2	0.954	0.955	0.962	0.944
	$RMSE$	0.033	0.021	0.034	0.104
	$ERRSQ$	0.219	0.422	1.215	1.593
Sips	K_S (l g ⁻¹)	0.042	0.081	0.031	0.044
	Q_S (mg g ⁻¹)	31.152	30.528	29.471	40.143
	n_S	0.943	0.052	1.232	1.621
	R^2	0.977	0.953	0.951	0.962
	$RMSE$	0.037	0.088	0.044	0.492
	$ERRSQ$	0.204	0.394	1.032	1.042

Table S7. Isotherm parameters and error deviation data for the adsorption of Co²⁺, Zn²⁺, Ni²⁺ and Cr³⁺ onto nPMMA_{SP}.

Model parameters	Co ²⁺ retention capacity (mg g ⁻¹)	
	-20%	+20%
Langmuir		
Q_0 (mg g ⁻¹)	30.448	30.977
K_L (l mg ⁻¹)	30.545	30.757
Freundlich		
K_F	30.656	30.757
n	30.541	30.855
Temkin		
b_T	33.785	31.583
A_T (l g ⁻¹)	32.882	31.555
Redlich-Peterson		
K_R (l g ⁻¹)	31.782	31.733
a_R (mg ⁻¹)	30.557	30.463
g	32.188	32.056
Sips		
K_S (l g ⁻¹)	30.555	30.146
Q_S (mg g ⁻¹)	30.505	30.478
n_S	31.035	30.862
Pseudo-first-order		
k_1	30.066	30.212
q_e	30.882	31.044
Pseudo-second-order		
k_2	30.062	30.015
q_e	30.112	30.026
Elovich		
α	33.565	31.511
β	32.805	31.152
Intraparticle diffusion		
k_d	32.647	31.505
C	31.893	31.051

Table S8. Parametric sensitivity of the model parameters for Co²⁺.

Metal ions	ΔH° (kJ mol ⁻¹)	ΔS° (J mol ⁻¹ K ⁻¹)	ΔG° (kJ mol ⁻¹)		
			303 K	313 K	323 K
Co²⁺	-18.966	-43.554	-3.556	-3.462	-2.401
Zn²⁺	-8.932	-33.442	-0.205	-0.202	-0.183
Ni²⁺	-10.882	-34.823	0.321	0.308	0.253
Cr³⁺	-13.185	-38.171	0.781	0.713	0.582

Table S9. Thermodynamic parameters for the metal ions sorption onto nPMMA_{SP}.